Original Paper

Cells Tissues Organs

Cells Tissues Organs 2000;167:106–120 Accepted after revision: December 23, 1999

Effect of Mechanical Load on Articular Cartilage Collagen Structure: A Scanning Electron-Microscopic Study

Max J. Kääb[a,b] Keita Ito[b] Berton Rahn[b] John M. Clark[d] Hubert P. Nötzli[c]

[a]Charité, Department for Trauma and Reconstructive Surgery, Humboldt University, Berlin, Germany;
[b]AO Research Institute, Davos, and [c]University Clinic for Orthopaedics, Balgrist, University of Zurich, Switzerland;
[d]Department for Orthopaedic Surgery, University of Washington, Seattle, Wash., USA

Key Words
Morphology · Loading, mechanical · Collagen fibers · Scanning electron microscopy · Cryofixation · Freeze substitution · Rabbit

Abstract
Little is known about the morphological effect of a mechanical load upon articular cartilage. The objective of this study was to describe and quantify the deformation of the articular cartilage collagen structure of the tibial plateau under static loading. Whole intact rabbit knee joints were loaded in vitro by simulating a quadriceps force of 3×, 1× or 0.5× body weight (high, medium, low) over durations of 30 or 5 min (long, short). Specimens were cryopreserved while under load and prepared for morphological evaluation by field emission scanning electron microscopy. Under high force and long duration loading the collagen fibers exhibited high deformation with an increased thickness of the layer of collagen fibers oriented almost parallel to the surface and a cartilage thickness reduced to 54%. Collagen fiber deformation occurred mostly in the transitional and upper radial zone. The area of tibial indentation and the cartilage thickness reduction increased with magnitude and duration of load. The collagen matrix did show a bulging edge at the border of the meniscus and exhibited remarkable deformation under the meniscus.

Abbreviation used in this paper

SEM	scanning electron microscopy

Introduction

Articular cartilage is a highly organized and specialized connective tissue. It consists of hydrated proteoglycans embedded within a dense network of collagen fibrils. This structure serves to transmit joint loads while minimizing contact stresses. The collagen network helps to determine the cartilage shape and cartilage mechanical properties.

The effects of mechanical loading on articular cartilage have been defined in numerous mechanical or biochemi-

KARGER
Fax + 41 61 306 12 34
E-Mail karger@karger.ch
www.karger.com

1422–6405/00/1673–0106$17.50/0

Accessible online at:
www.karger.com/journals/cto

Max J. Kääb, MD, PhD, Charité University Clinic
Clinic for Trauma and Orthopaedic Surgery, Humboldt University Berlin
Campus Virchow Klinikum, Augustenburger Platz 1, D–13353 Berlin (Germany)
Tel. +49 30 450 50, Fax +49 30 450 52901
E-Mail max.kaeaeb@charite.de, http://www.charite.de/unfallchirurgie

Table 1. Distribution of specimens

	Load magnitude/duration				
	3 × BW 30 min high/long	1 × BW 30 min medium/long	0.5 × BW 30 min low/long	3 × BW 5 min high/short	1 × BW 5 min medium/short
	10/0/4	5/0/2	5/0/2	5/0/2	5/0/0
Recovery (+2/+4/+16/+30 min)	4/0/0	4/0/0			
Unloaded	10/5/5				

Numbers of rabbit knee joints prepared for each method are shown: cryofixation (SEM)/conventional aqueous fixation (SCM)/light microscopy. Load magnitudes: high (3 × BW), medium (1 × BW), low (0.5 × BW); load duration: long (30 min), short (5 min). BW = Body weight.

cal studies [Hayes et al., 1972; Mow et al., 1980; Oloyede and Broom, 1994; Tepic and Ito, 1997]. Alternatively light microscopy or scanning electron microscopy (SEM) has been used to study the morphological effects of mechanical loading on the cartilage matrix [McCall, 1969; Broom and Myers, 1980; Takei et al., 1986; O'Connor et al., 1988; Glaser and Putz, 1996; Kobayashi et al., 1996]. SEM has been particularly useful to demonstrate alterations in the three-dimensional arrangement of the cartilage collagen structure to mechanical loading. Phenomena such as surface roughening, denser packing of collagen fibers and crimping of fibers were found to result from mechanical loading. However, most of these studies used excised samples of articular cartilage rather than intact joints. Moreover, the direct response of the collagen matrix to load was not observed and quantified. A more detailed knowledge of joint morphology under physical stress is essential for understanding normal function and degeneration of articular cartilage.

In our previous work [Nötzli and Clark, 1997; Kääb et al., 1998a] deformation of collagen fibers in the rabbit tibial plateau cartilage under static and cyclic loads was analyzed. There it was shown that cartilage deforms significantly less under cyclic loads compared to static loads. Now we tried to answer the question of how the collagen structure deforms under different magnitudes and durations of a mechanical load. Specifically, we analyzed and quantified the three-dimensional deformation of the collagen structure and its relation to the meniscus within whole knee joints loaded under static compression.

Methods

Sample Preparation and Mechanical Loading

Forty-six adult female New Zealand White rabbits (mean body weight 4.1 kg, age 10–13 months) were euthanized. Knee joints were harvested by transection at the proximal femur and the distal tibia. Soft tissue and muscles were removed from each knee, and care was taken not to damage the knee joint ligaments or to open the joint capsule. Radiographs were examined for assessment of skeletal maturity and to exclude joint deformities.

A simple loading device for static load application was used for in vitro testing of rabbit whole knee joints [Nötzli and Clark, 1997; Kääb et al., 1998a]. The load was applied by simulating quadriceps tension through a wire, attached to the proximal patella through a horizontally drilled hole. The knee was maintained at a fixed 90° flexion position for loading. Static loads of 3×, 1× or 0.5× body weight (high, medium, low force) were applied to the knee joint for time periods of 30 or 5 min (long, short duration) (table 1). The wire tension was generated using a testing machine (Mikrotron 654, testing machine, Russenberger & Müller, Schaffhausen, Switzerland), and the magnitude of the force controlled by a load cell. While loading, the specimens were submerged in isotonic saline solution (ph 7.4 buffered Ringer solution). Unloaded knee joints served as controls. To determine the rate of recovery after unloading the joints were removed from the load and held for either 2, 4, 16 or 30 min prior to cryofixation (table 1).

Sample Preservation

A previously developed protocol [Nötzli & Clark, 1997; Kääb et al., 1998a] was used for cryofixation of the entire knee joint. The samples were frozen while under load by immersion into isopentane slush, precooled with liquid nitrogen to below –160°C for 4 min. Samples were then removed from the loading device and fixed by freeze substitution. Initial fixation (in a mixture of 10% acrolein, 0.2% tannic acid in 30% methanol and 58.8% acetone) was performed at –80°C for 7 days. Samples were then transferred into a second fixation solution (5% glutaraldehyde, from a 50% aqueous solution, in 10% methanol and 85% acetone) and maintained at –23°C for 4 days. The temperature was then increased to 4°C for

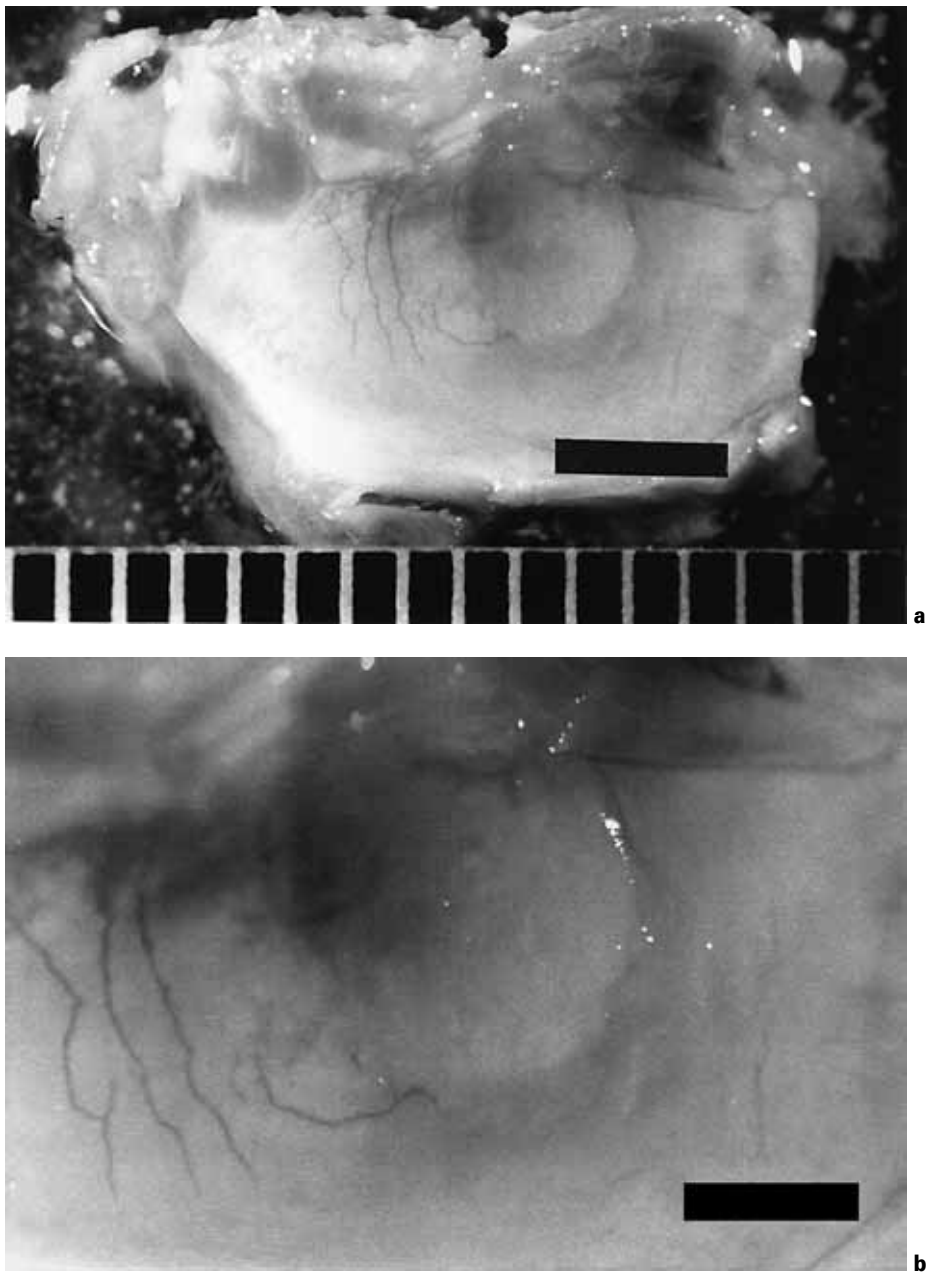

Fig. 1. Medial tibial plateau surface with the femoral indentation in the cartilage after freeze fixation (high-force, long-duration loading). **a** Clear circumference of the indentation. Bar: 3 mm. **b** Clefts more outside the indentation. Bar: 1.5 mm.

24 h. The samples were then transferred into 100% ethanol. The joints were carefully opened and the tibial plateau was cut away, leaving approximately 1 mm of subchondral bone attached. The trimmed plateaux were then postfixed in 1% osmium tetroxide in 100% ethanol for 120 min at 49 °C.

After fixation, a freeze fracture of the tibial plateau perpendicular to the articular surface was made through the middle of the indentation [Humphreys et al., 1974]. The samples were dried using a Polaron E3000 critical point drier (Agar Scientific, Essex, UK), using CO_2 as a transitional medium. Specimens were coated with 8 nm of gold in a Baltec MED 020 unit (Baltec, Balzers, Liechtenstein) and examined with a Hitachi S-4100 field emission SEM (Hitachi, Tokyo, Japan). For imaging the collagen structure of a few specimens at higher magnification, backscattered electron imaging at high emission currents was used [Richards and Gwynn, 1995]. The main location of interest of the study was the medial tibial plateau. The images were stored digitally with an image management system (Quartz PCI, Quartz Imaging, Vancouver, Canada).

Unloaded samples – as controls for fixation artifacts due to cryofixation – were fixed within an aqueous, buffered solution of 2.5%

glutaraldehyde with 4% paraformaldehyde for 4 h [Richards and Kääb, 1996]. Each fixed sample was dehydrated using graded ethanol solutions. Once samples had been dehydrated, the procedure was followed as described above.

Additional samples were prepared for light microscopy. The samples were loaded, frozen, fixed, dehydrated and brought to room temperature (using the cryomethod as described above), rinsed in 100% ethanol for 3 days and placed into 100% xylol before infiltration and embedding in methyl-methacrylate. Polymerization was done for 48 h at 32 °C. Sections were cut to 200 µm thickness in the frontal plane with a Microtome (Sawing Microtome 1601, Wetzlar, Germany) and polished (Polishmachine Stähli-Lapp, Stähli, Biel, Switzerland) to 80 µm thickness. The sections were stained with Azan to highlight the collagen fibers [Romeis, 1989].

Evaluation

Using a photomacroscope the tibial plateau surface was examined. More detailed morphological observations were made by light microscopy and SEM. The samples were evaluated for the quality of fixation (shrinkage artifacts, collagen fibers) and analyzed for the arrangement of the collagen structure. The parameters evaluated were the bending pattern and crimping waves of collagen fibers, cleft formation in the cartilage surface, condylar indentation and indentation under the meniscus.

In loaded points, the femoral condyle creates a discrete indentation in the tibial plateau (fig. 1). The area of this tibial indentation was measured before the sample was freeze-fractured. To measure the area of tibiofemoral indentation, the sample was immersed in 100% ethanol to prevent drying effects. The cartilage surface was viewed under a stereomicroscope (Wild, Heerbrugg, Switzerland) at a magnification of 12.5 ×. The outer contours of cartilage indentation were traced with a cursor on a digitizing table (Kontron Electronics, Munich, Germany) where the cursor was projected into the sample in the field of view. The area (mm^2) was calculated and recorded.

For each sample the deformation of the collagen in the tibial plateau was quantified by measuring the minimum cartilage thickness after loading and the period of collagen fiber crimping based on SEM images utilizing an image analysis and measurement program (PC-Image, Foster Findlay, Newcastle, UK). Only fractures through the middle 15% of the indentation of the tibia plateau were used for quantitative evaluation, controlled by stereomicroscopy. The minimum cartilage thickness in the tibial plateau after loading (distance from the surface to the subchondral bone, at a right angle to the surface) was measured from calibrated SEM images. This was then compared with the unloaded cartilage thickness of the same sample derived by repeated (to minimize measuring error) tracing of a collagen fiber bundle from the calcified cartilage/deep zone interface to the articular surface. The reduced cartilage thickness was expressed as a percentage of the initial cartilage thickness. All comparisons were analyzed using the Ryan-Einot-Gabriel-Welsch (REGQW) multiple range test at a significance level of $p = 0.05$. The maximum fiber crimp wavelength in the center of the indentation was measured (in µm). The parameters of indentation area and cartilage thickness were examined with respect to recovery. No statistical tests were performed for fiber crimp comparisons.

Results

Cartilage Surface/General Findings

Well-defined indentations in the tibial plateau were clearly seen in the central tibial plateau near the intercondylar tubercle for all modes of loading (fig. 1a). A sharply defined indentation ridge caused by the internal meniscal edge was also observed. The unloaded controls exhibited no indentations. A few clefts of approximately 40 µm width and maximum 2 mm length were visible in the cartilage surface of the medial tibial plateau (fig. 1, 2a). These fissures were located in areas outside of the femoral indentation after high and medium magnitude and long duration load (fig. 1b). After low-force and short-duration loading these clefts were visible as well but showed no specific distribution. The cryofixation method resulted in a well-preserved collagen structure when analyzed under SEM, comparable to the samples fixed by conventional chemical fixation. The only morphological difference in the cryofixed samples were the segregation artifacts in the chondrocyte ultrastructure due to ice crystal formation during freezing (fig. 3c).

Morphology

In the unloaded samples, fibers ran exclusively vertical and perpendicular from the calcified cartilage to the articular surface (fig. 4). In the loaded knee joints the collagen fibers showed a characteristic pattern of bending which varied. After high force and long duration loading, the collagen fibers exhibited bending in the loaded areas, forming a characteristic layer with collagen fibers lying almost parallel to the surface. The maximum thickness of this layer was at the center of the indentation and was approximately one third of the loaded cartilage thickness (fig. 3, 5). In the lower deep/radial zone the fibers indicated much less deformation (fig. 3a, b). Under low force

For Figure 2a–d see pages 110/111

Fig. 2. All images are from the same sample. **a** Imprint of the femur (C) condylus (high-force, long-duration load): raised bulging edge (B) at the border femoral imprint and where the meniscus (M) was removed. Bar: 200 µm. **b** There is also significant deformation under the meniscus. The collagen fibers (dashed line) can be traced into the edge. The height of the bulging edge is indicated by an arrow. Bar: 90 µm. **c** Chondrocytes (arrows) in the edge and structured edge. Bar: 30 µm. **d** Appearance of fibrous matrix in the backscattered electron mode at high magnification. Bar: 3 µm.

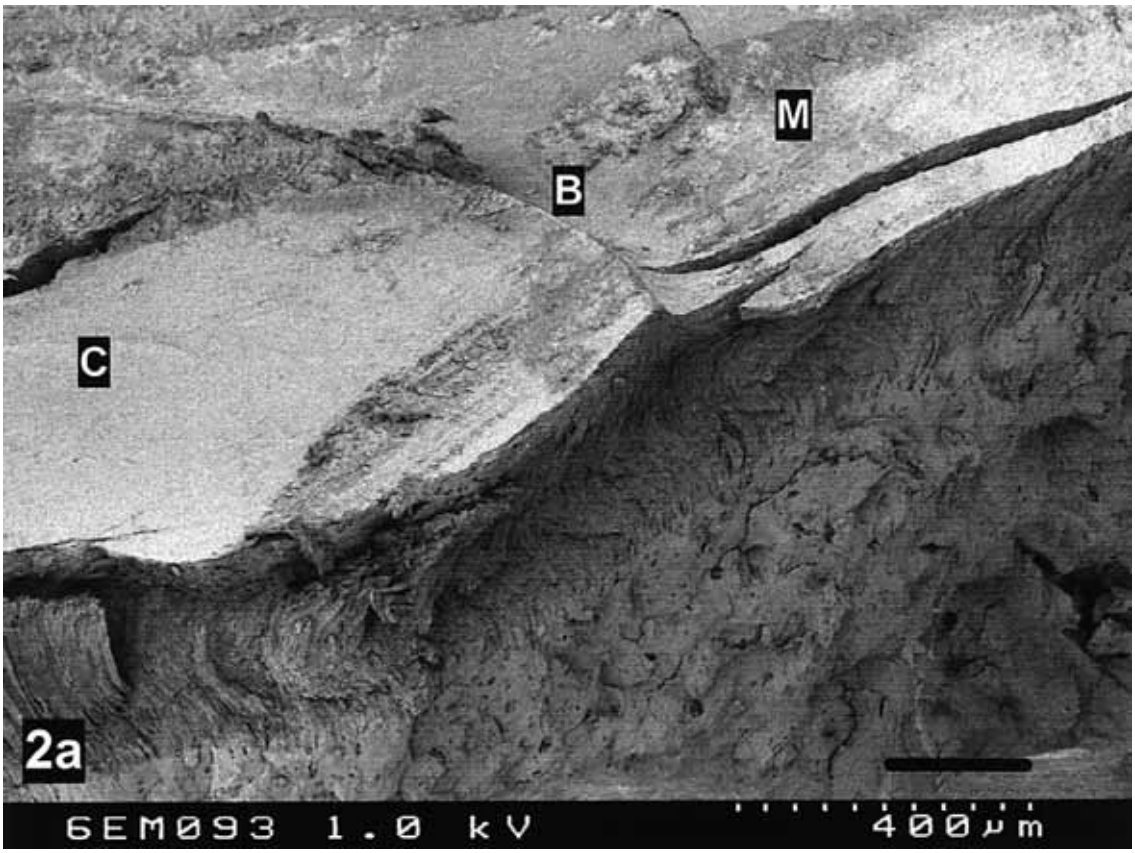

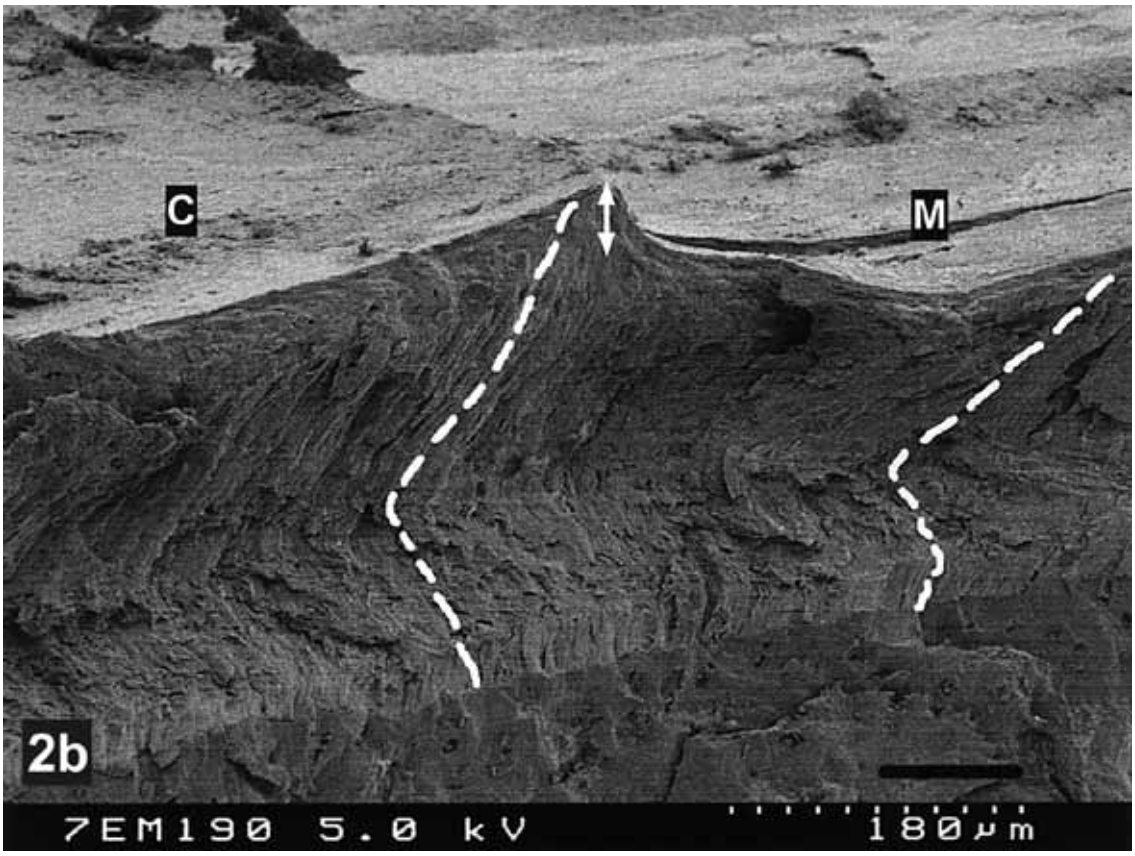

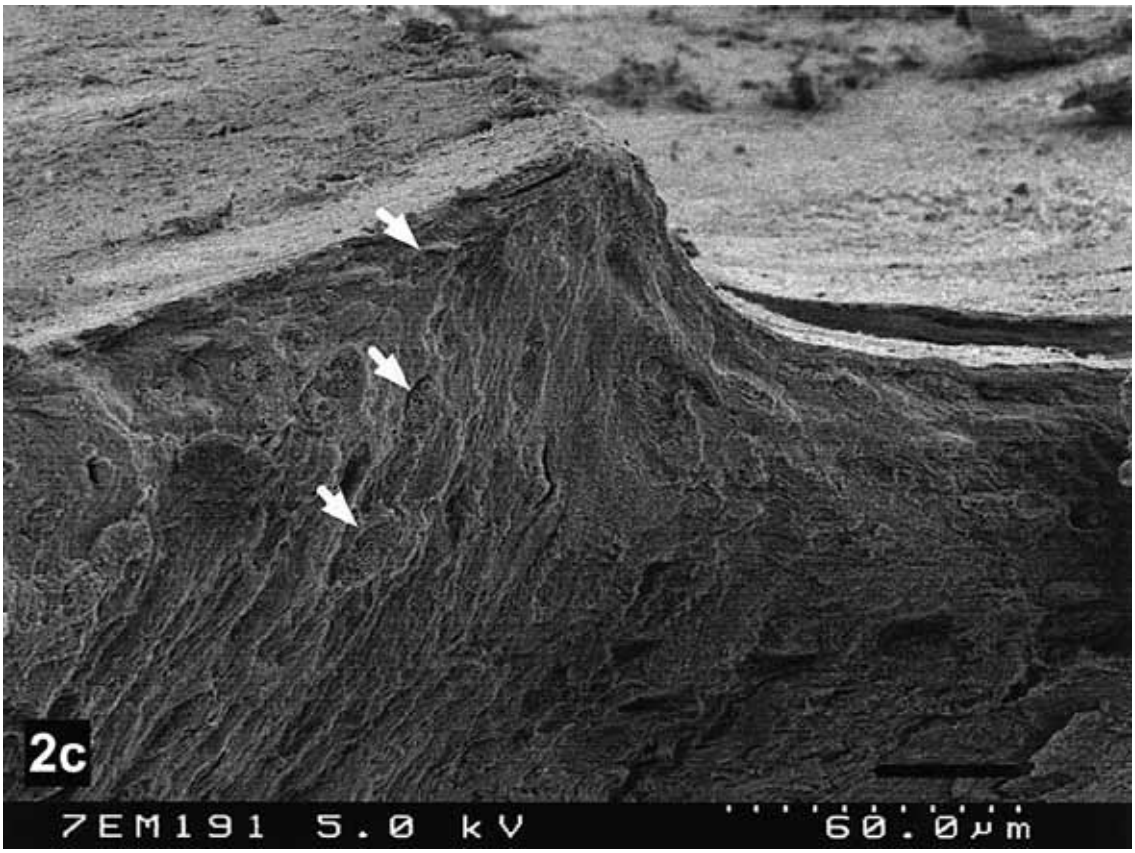

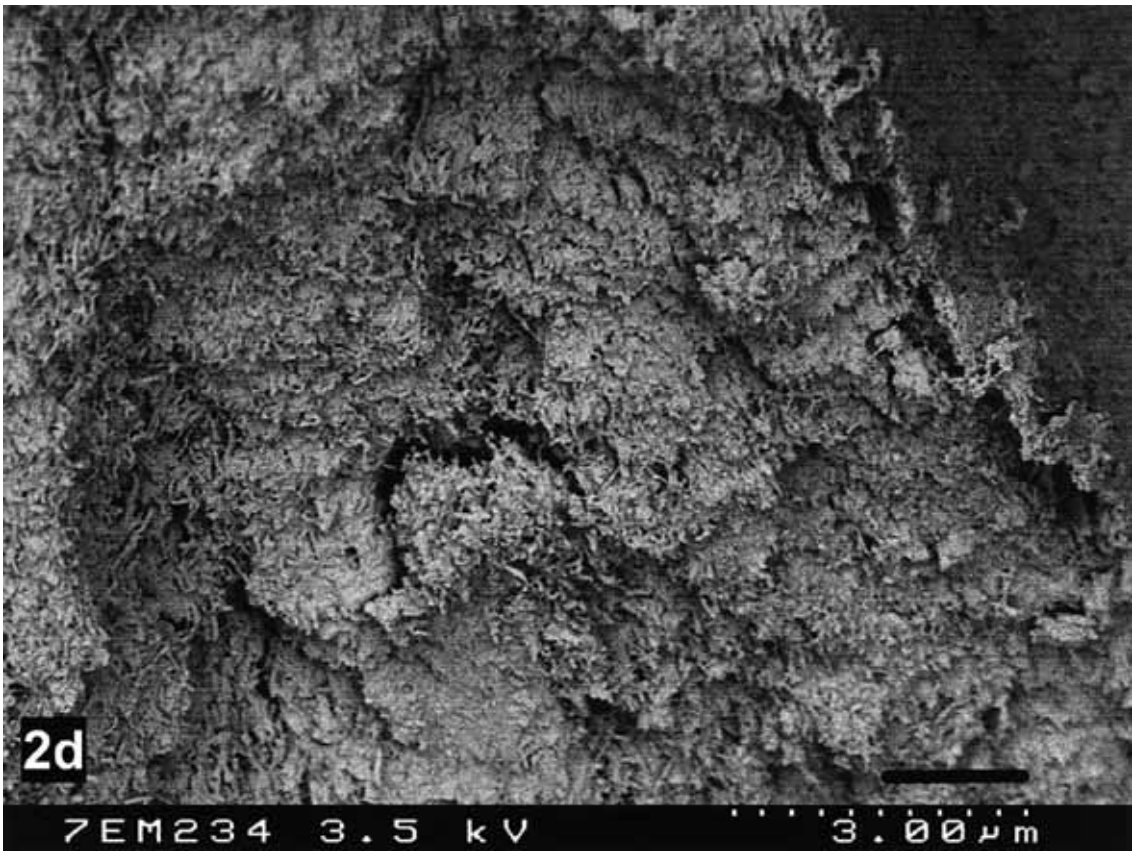

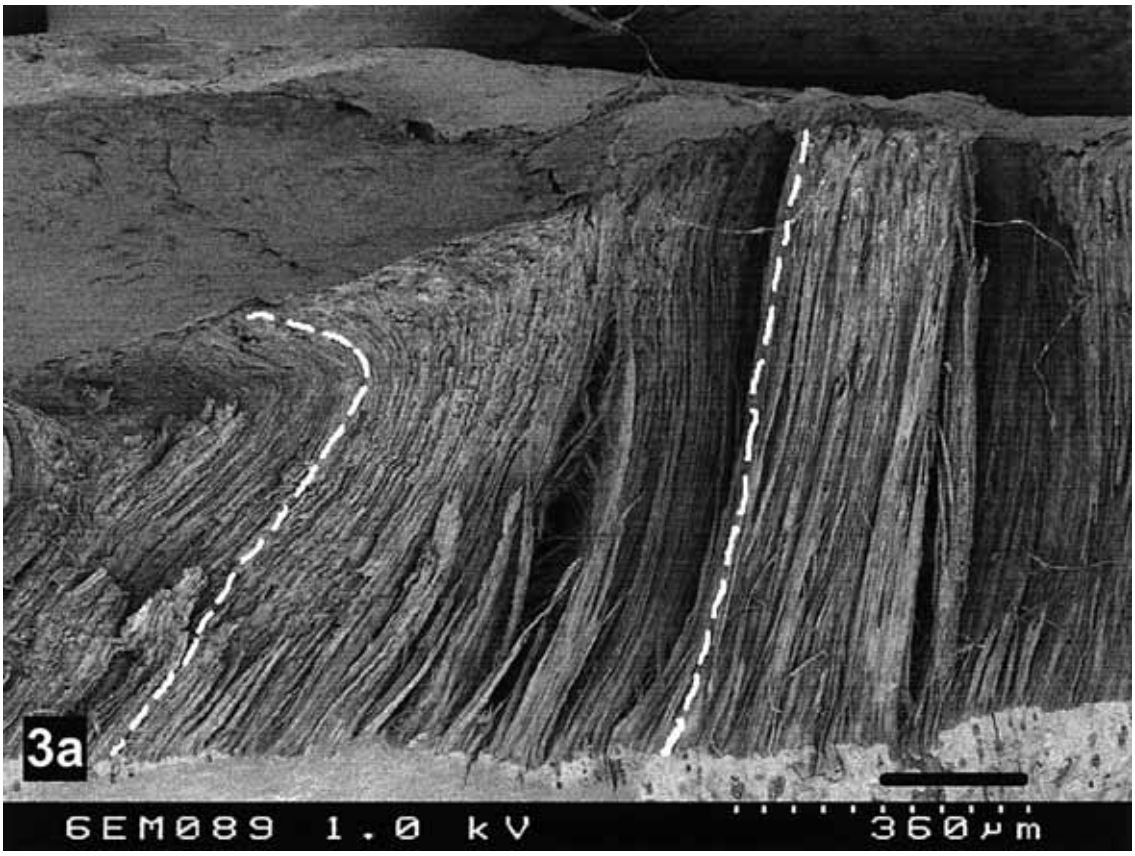

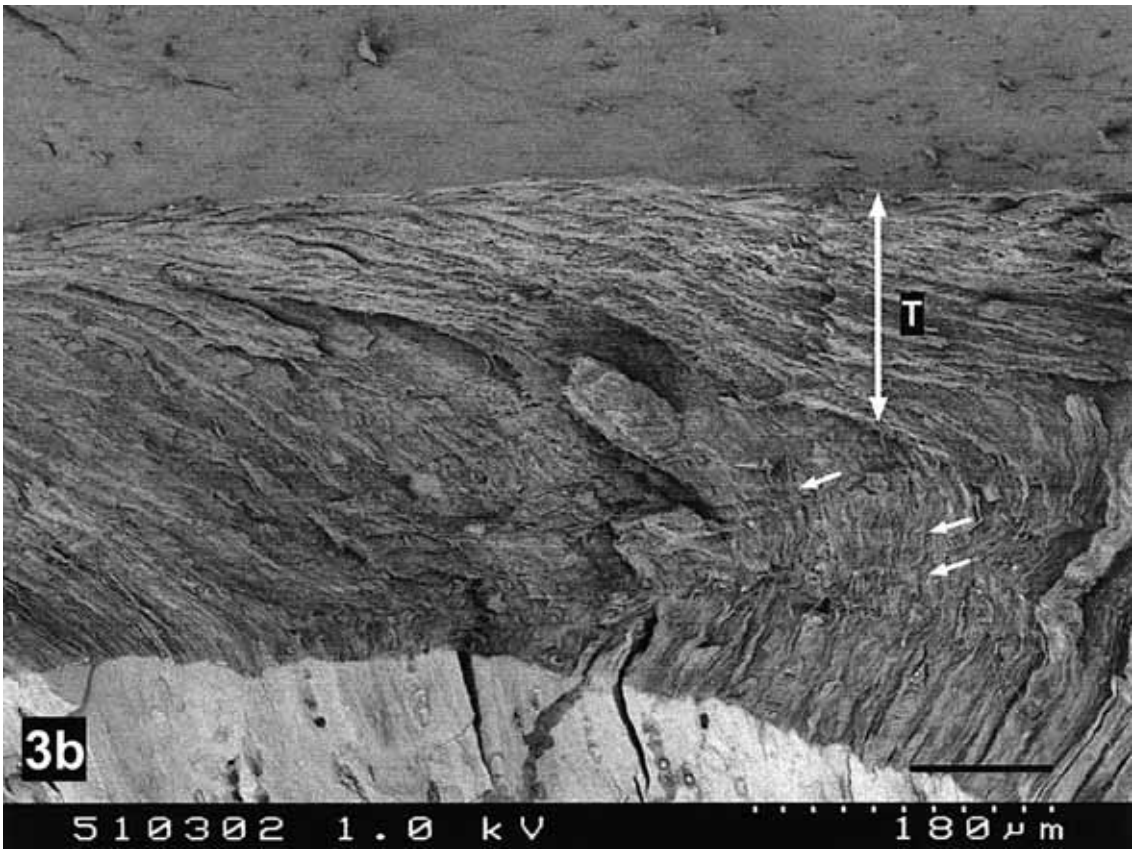

Fig. 3. Middle magnification of the same samples as in figure 5. **a** Lateral aspect of the sample with the border-deformed/undeformed fibers (dashed lines). Bar: 180 µm. **b** Middle of the indentation. Tangential layer (T) formed by fibers lying parallel to the cartilage surface. Fiber crimp in the the upper radial zone (arrows). Bar: 90 µm. **c** Fiber crimping in the center of the indentation at the border upper/lower radial zone. Chondrocytes (arrows) with segregation artifacts (due to ice crystal damage). Bar: 20 µm.

and long duration loading the collagen fibers were oriented at an acute angle to the surface (fig. 6). Under low-force and short-duration loading no increased tangential layer was formed. The highest degree of bending of all the different loading cases was observed in the center of the indentation under the condyle, with increasingly less bending towards the periphery (fig. 3a, 5). Beneath the meniscus a lower degree of bending was observed, without forming a layer of collagen fibers parallel to the surface (fig. 2b). Furthermore, no surface fibrillation, damage of the surface layer or sign of splitting of the subchondral bone/cartilage interface was found in any loading cases. Collagen fiber bending and crimping were visible under light microscopy as well (fig. 7).

At the border of the femoral and meniscal indentation there was a raised edge around the condylar indentation after high and medium long duration loading (fig. 2a, b). The edge had a maximum height of 50 µm. This rim was formed by collagen fibers. The collagenous structure continued from the radial zone to the surface of this edge (fig. 2c). At higher magnification, deformed chondrocytes appeared within the edge. The matrix appeared to have a fibrous structure (fig. 2d). Under low-force or short-duration loading, no such edge was detected.

Some collagen fibers exhibited a regular sinusoidal crimp under medium- and high-force, long-duration loads. This crimp was visible only in regions of indentation and was most prominent at the center of the indentation and in the deeper zones (fig. 3b, c). Little or no crimp was observed in the segment of the fibers running parallel to the surface. Instead crimping was found between the upper and lower radial zone (fig. 3b). After

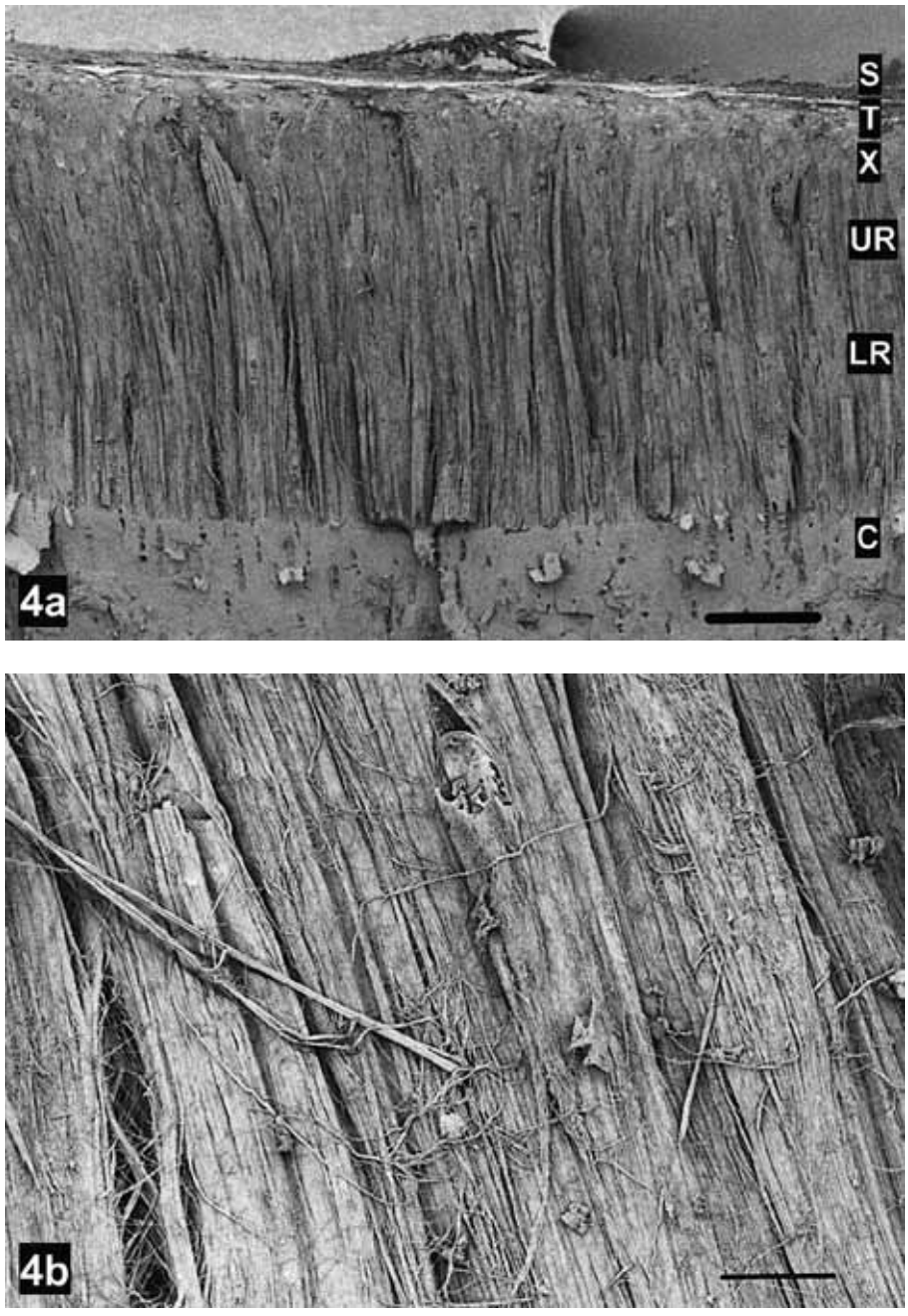

Fig. 4. Unloaded central tibial plateau. Fibers show no deformation. **a** S = Surface; T = tangential; X = transitional; UR = upper radial zone; LR = lower radial zone; C = calcified zone. Bar: 150 μm. **b** Parallel running collagen fibers in the radial zone show no signs of deformation. Bar: 20 μm.

high loads, a crimp was present in collagen fibers beneath the meniscus. No crimping was detected in unloaded samples.

Quantitative Data

There were significant differences due to load duration (30 vs. 5 min) only at medium but not at high loads ($p < 0.05$). After long-duration loading there was a difference between medium and low force (9.4 ± 0.8 vs. 7.4 ± 1.1 mm^2, $p < 0.05$, fig. 8). There was no significant difference between high and medium force for long-duration loading but there was under short-duration loading (10.1 ± 1 vs. 7 ± 0.04 mm^2, $p < 0.05$). Under short-duration loading the area was significantly different between high

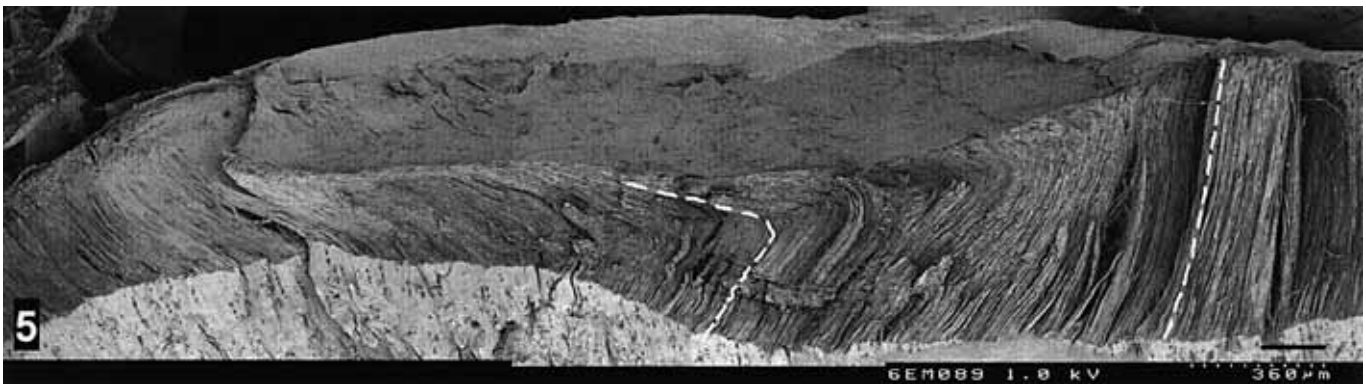

Fig. 5. SEM photograph with a fracture through the middle of the indentation of tibial plateau (high force, long duration). The indentation and collagen fiber bending are visible. On the right handside no bending and increasing deformation to the middle of the indentation. Bar: 400 µm.

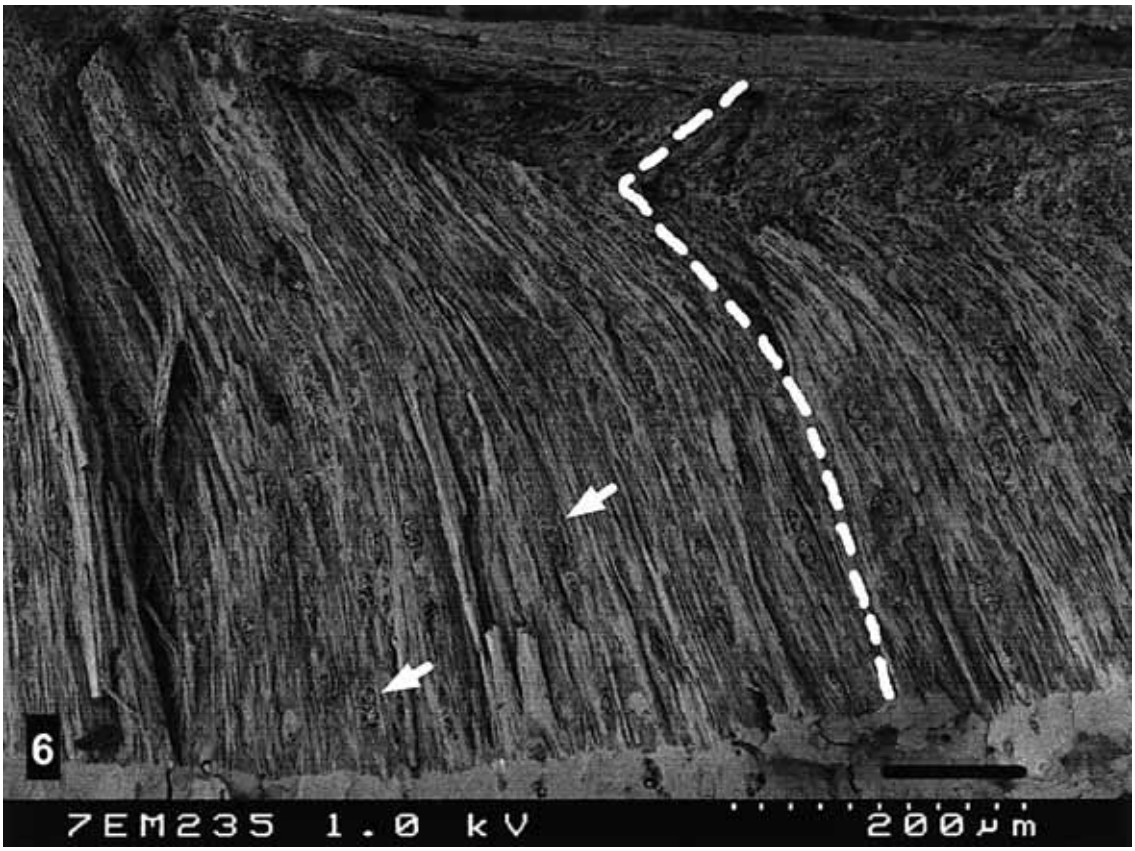

Fig. 6. Deformation under low and long load in the center of indentation of the condylus. The collagen fibers show a sharp bending (acute bending angle) in the upper one fourth of the cartilage layer. A single collagen fiber (dashed line) and chondrocytes (arrows) are indicated. Bar: 100 µm.

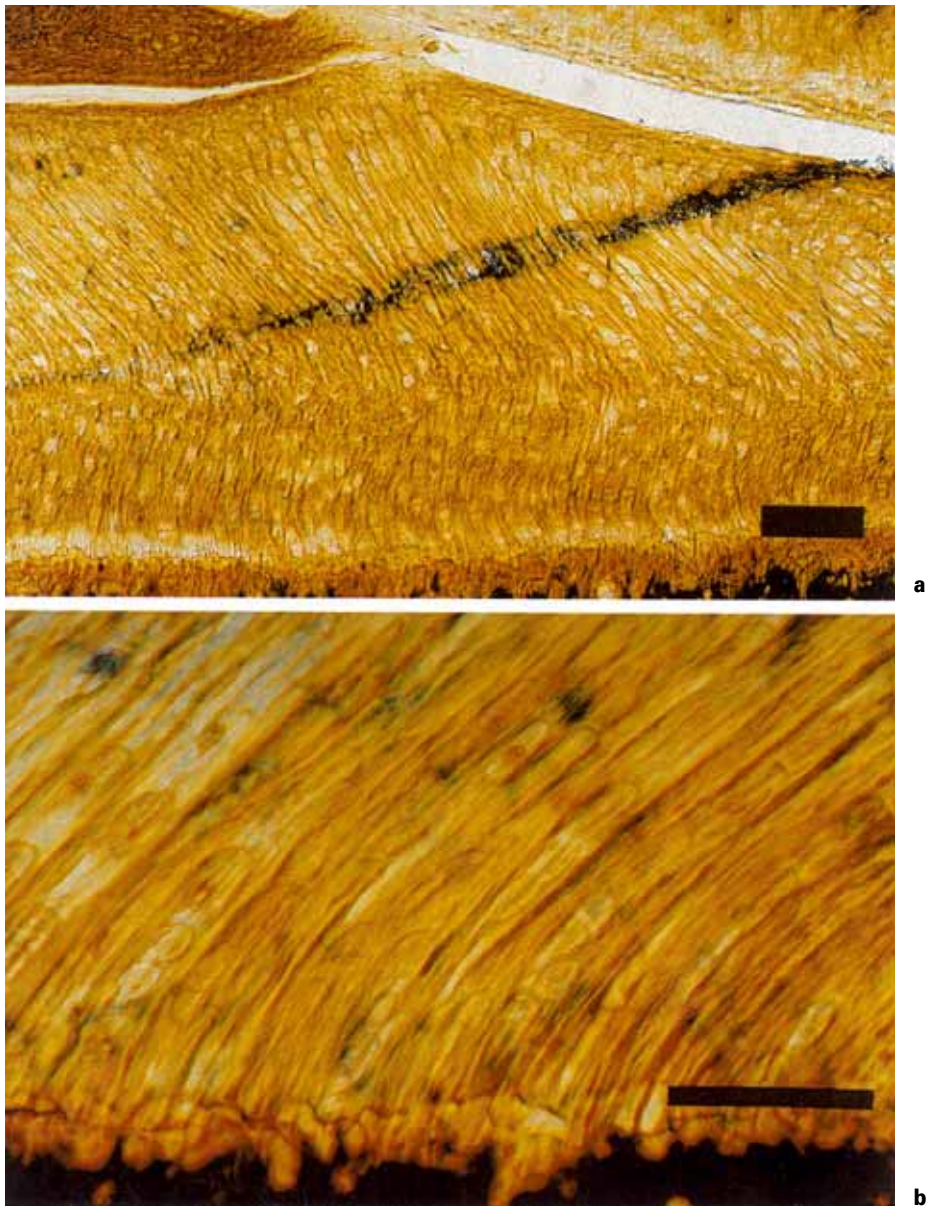

Fig. 7. Light microscopy of loaded cartilage (high force, long duration). The slight lift-off of the meniscus is an artifact due to histological preparation. **a** Indentation, bending and crimping of collagen fibers under the condylus and meniscus. Bar: 100 µm. **b** Fiber bending at the border calcified cartilage, radial zone. Bar: 50 µm.

and medium force ($p < 0.05$). Within 16 min the indentation area was completely recovered after both high and medium force. After 4 min of unloading in both cases the indentation was still 9.4 mm^2 (± 0.4; high force) and 7.6 mm^2 (± 0.4; medium force).

Thickness of the cartilage in the center of indentation was related to load magnitude and duration and more reduced with higher and longer loads (fig. 9). After a short-duration load the thickness was significantly greater for both high- and medium-force loads when compared to long-duration loads (78 ± 2 vs. 54 ± 3%, $p < 0.05$ for high-force loading). The effect of load magnitude on cartilage thickness was significant for all load cases ($p < 0.05$). The higher the load, the more the cartilage thickness was reduced. Under long-duration loading the remaining cartilage thickness after high-force loading was 54% (± 3) compared to 84% (± 1.7) after low-force loading. The cartilage thickness recovered completely within 30 min after high-force loading. After 16 min without load the remaining cartilage thickness was 89% (± 3.6) after high-

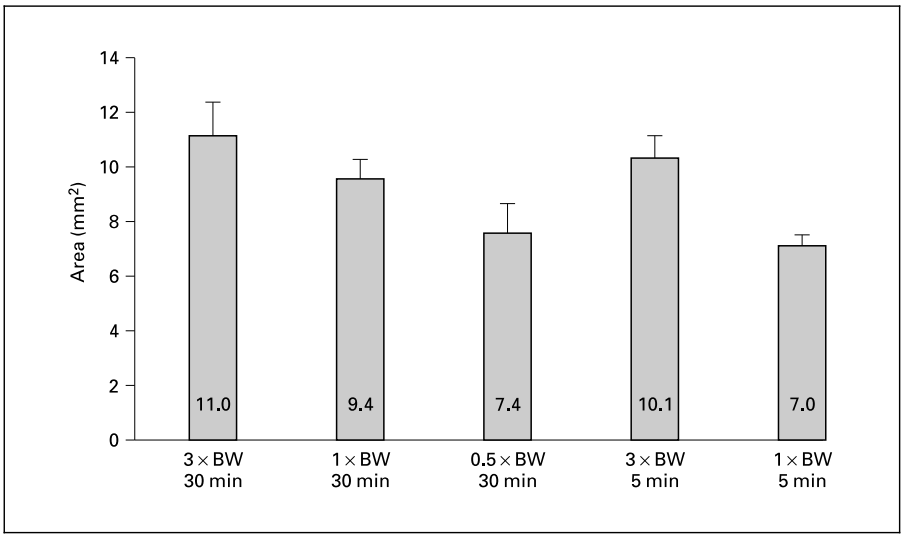

Fig. 8. Area of tibial identation. Significance of magnitude of load ($p < 0.05$) and duration of load ($p < 0.05$). BW = Body weight.

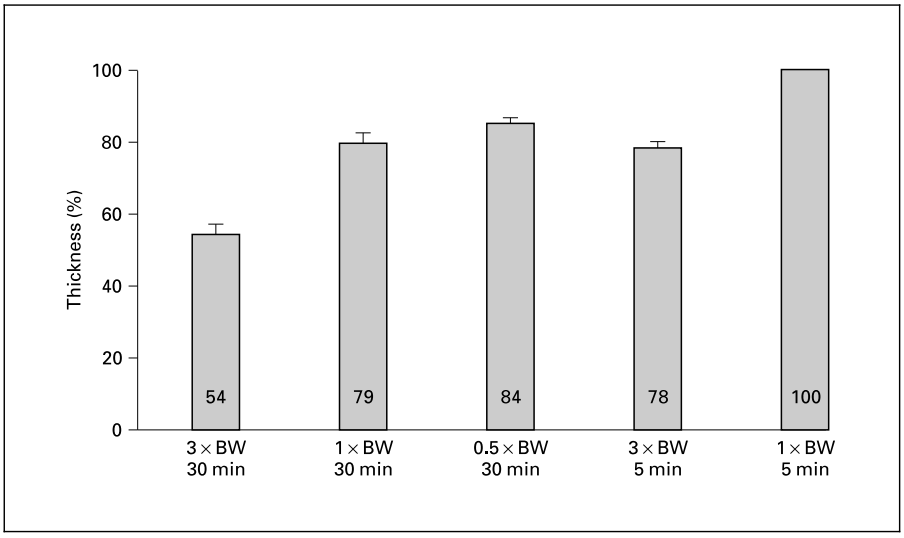

Fig. 9. The remaining cartilage thickness at the center of the indentation after loading.

force loading while after medium-force loading it was not reduced.

The collagen fiber crimp was also dependent on duration and magnitude of load. The higher the magnitude and the longer the duration of the load the shorter was the crimp wavelength. After long-duration loading the crimp wavelength was 6 µm (± 0.8) after high-force loading. After low loading it was 17 µm (± 0.5). After high-force and short-duration loading the crimp was 16 µm (± 1.1). The collagen recovered completely from crimping for all loading cases.

Discussion

Using a loading-freezing technique, the cartilage collagen structure of whole joints was preserved while under load. Mechanical loading led to significant deformation of the collagen structure from the surface to the deep zone and this deformation was dependent on magnitude and duration of load.

Methodology

The challenge to everyone wishing to study the morphology of loaded cartilage is to maintain the loaded configuration through subsequent steps of preparation, neces-

sary for microscope preparation. One approach for this purpose is cryoscanning electron microscopy, a technique that allows excellent preservation of tissue close to its natural state while under load [Kabayashi et al., 1995, 1996]. This method is thought to reduce artifacts caused by fixation and drying. However, the size of the specimen to be examined is limited to only few cubic millimeters. Other methods used aldehyde chemical fixation [McCall, 1969; Glaser and Putz, 1996], direct light microscopy of hydrated cartilage [Broom and Myers, 1980; O'Connor et al., 1988] and acrylic casting of loaded samples have a great potential for artifact creation [Simon et al., 1973; Fukubayashi and Kurosawa, 1980]. In addition, the three-dimensional structure cannot be observed by SEM. Cryopreservation of specimens while under load, by placing the sample together with the loading apparatus into a deep freezer has been used previously [Takei, 1979]. However, due to the slow heat transfer rates involved, this approach was not suitable for the simulation of physiological loading conditions. With our method of plunge freezing in isopentane slush, the temperature inside the knee joint reached –25°C within 30 s and outside the joint (ligaments and capsule) within a few seconds. Subsequent fixation was performed by freeze substitution [Nötzli and Clark, 1997; Kääb et al., 1998a]. In the unloaded state the articular cartilage shape is determined by the collagen matrix that constrains swelling generated by hydration of the proteoglycans. The goal of this method was to preserve loss of water and proteoglycans. No damage to overall collagen structure was observed, although ice crystal artifacts were present in the chondrocyte ultrastructure [Richards and Kääb, 1996]. However, this was inconsequential, since ultrastructural observations of the cell and its matrix were not within the scope of this study. In addition we chose a loading condition, which we believe is approximately physiological [Nötzli and Clark, 1997]. Although the high-load levels were extreme, their use was necessary in order to show differences in collagen deformation under significantly different circumstances. Although the exact tibiofemoral joint reaction forces generated by the device were not measured, the forces were applied in a standardized, reproducible manner.

Matrix Deformation

One of our main morphological findings was the bending deformation of collagen fibers under load. An alignment of fibers at right angles to the direction of load and a denser packing of collagen fibers has been observed by other authors [McCall, 1969; Glaser and Putz, 1996, Kobayashi et al., 1996; Langsjö et al., 1999]. McCall [1969] observed fibers remaining in their deformed positions after unloading. We did not find any permanent deformation or damage due to loading or any areas of unrecovered cartilage. Within 30 min the cartilage recovered completely. Perhaps this could be attributed to the more physiological environment used in our study. In this case the femoral condyle acts as a physiological indenter compared to an artificial steel indenter. The recovery of the tissue is in accordance with biomechanical data on the biphasic behavior of an articular cartilage under load [Kempson et al., 1971; Mow et al., 1982, 1989].

We also demonstrated the deformation of the cartilage matrix, forming a bulging edge under extreme loads and a special relation to the meniscus. The bulging edge has been described in the literature and is thought to be composed of an amorphous material without a collagen fibril network and probably due to large globular glycoproteins precipitated from the synovial fluid [Maroudas, 1976; Orford and Gardner, 1985; Kobayashi et al., 1995, 1996]. In our study the bulging edge was visible only under high-force and long-duration load and appeared at higher magnification to be composed more of a fibrillar structure than an amorphous structure. Within the bulging edge segregated chondrocytes (due to ice crystal formation) were also visible. The difference to the findings of Kobayashi et al. [1995, 1996] might be explained by the fact that we used a more physiological loading situation of a whole joint with meniscus and an unstructured surface. Under extreme loading, the cartilage might fill some free space in the border tibial cartilage, condyle and meniscus due to different material properties of these interfaces [Proctor et al., 1989; Fithian et al., 1990]. The bulging edge may also demonstrate that the surfaces become more congruous at high loads [Simon et al., 1973].

The crimped waveform of the collagen matrix under mechanical loading has also been observed previously [McCall, 1969; Broom and Myers, 1980; Poole et al., 1984; Glaser and Putz, 1996]. Broom and Myers [1980] also showed the complete recovery of the crimp after high compressive forces. We observed much less or no crimp under lower magnitude and shorter duration of load.

Fluid Movement

Articular cartilage is a biphasic material and its compressive, time-dependent behavior is the consequence of the flow of interstitial fluid [Mow et al., 1982]. We observed a characteristic formation of clefts around the indentation. We assume from the morphological findings that fluid is forced out of the main region of compression and moves into regions with lower pressure since most of

the water in articular cartilage is freely exchangeable in cartilage [Linn and Sokoloff, 1965; Maroudas and Venn, 1977]. Under lower and shorter loading there is less water movement into unloaded regions, since less deformation occurs. The clefts probably form during dehydration, and are presumably the result of tensile forces within the tissue caused by increased shrinkage in regions with a higher water content [Crang, 1988; Kääb et al., 1998b]. Weiss [1973] and others [Meachim and Bentley, 1978] viewed clefts in articular cartilage as an early ultrastructural characteristic of osteoarthritis. However, we believe that the clefts observed in our study are preparation artifacts and may not be markers of cartilage microdamage.

The mechanical load, to which the articular cartilage is exposed daily during the entire life span, seems to be a significant factor responsible for the maintenance of normal articular cartilage composition, structure and function. Articular cartilage plays an important role in reducing stress to an acceptable level within the joint system. Since increased stresses in the altered joint situation, e.g. following meniscectomy, lead to osteoarthrosis, it is important to know the morphological response of the cartilage collagen structure – the shape-maintaining part of cartilage – under normal increased stresses. Critical aspects of cartilage degeneration and injury may occur at the level of collagen structure.

More detailed knowledge of the morphology of joints under physiological loading conditions should lead to a better perception of the pathophysiology of mechanically induced joint diseases. It is necessary to analyze cartilage morphology under load to understand how the articular cartilage, which provides the normal function of a synovial joint, can be restored after damage, e.g. caused by degeneration, trauma and inflammation. An improved basic knowledge of cartilage morphology may help us to understand cartilage pathology and aid in the development and evaluation of new therapies for disease-affected cartilage.

Acknowledgements

This project was supported by a grant from the AO/ASIF Foundation, Switzerland No. 96-K56. The authors wish to thank W.C. Hayes, R.G. Richards, I. Gwynn, S. Ferguson, F. Eckstein and G. Owen for their comments.

References

Broom, N.D., D.B. Myers (1980) A study of the structural response of wet hyaline cartilage to various loading situations. Connect Tissue Res *7:* 227–237.

Crang, R.F. (1988) Artifacts in specimen preparation for scanning electron microscopy; in Crang R.F., K.L. Klomparens (eds): Artifacts in Biological Electron Microscopy. New York, Plenum Press, pp 107–129.

Fithian, D.C., M.A. Kelly, V.C. Mow (1990) Material properties and structure-function relationships in the menisci. Clin Orthop *252:* 19–31.

Fukubayashi, T., H. Kurosawa (1980) The contact area and pressure distribution pattern of the knee. A study of normal and osteoarthrotic knee joints. Acta Orthop Scand *51:* 871–879.

Glaser, C., R. Putz (1996) Changes in the collagenous architecture of articular cartilage during compressive loading lead to a two layer model. 10th Conference of the European Society of Biomechanics, Leuven, p 308.

Hayes, W.C., L.M. Keer, W. Herrmann, L.F. Mockros (1972) A mathematical analysis for identation tests of articular cartilage. J Biochem *5:* 541–551.

Humphreys, W.J., B.O. Spurlock, J.S. Johnson (1974) Critical point drying of ethanol-infiltrated cryofractured biological specimens for scanning electron microscopy. Scanning Microsc 275–283.

Kääb, M.J., K. Ito, J.M. Clark, H.P. Nötzli (1998a) Deformation of articular cartilage collagen structure under static and cyclic loading. J Orthop Res *16:* 743–751.

Kääb, M.J., H.P. Nötzli, J. Clark, I. Gwynn (1998b) Dimensional changes of articular cartilage during immersion-freezing and freeze-substitution for scanning electron microscopy. Scanning Microsc, in press.

Kempson, G.E., M.A.R. Freeman, S.A.V. Swanson (1971) The determination of a creep modulus for articular cartilage from indentation tests on the human femoral head. J Biochem *4:* 239–250.

Kobayashi, S., S. Yonekubo, Y. Kurogouchi (1995) Cryoscanning electron-microscopic study of the surface amorphous layer of articular-cartilage. J Anat *187:* 429–444.

Kobayashi, S., S. Yonekubo, Y. Kurogouchi (1996) Cryoscanning electron microscopy of loaded articular cartilage with special reference to the surface amorphous layer. J Anat *188:* 311–322.

Langsjö, T.K., M. Hyttingen, A. Pelttari, K. Kiraly, J. Arokoski H.J. Helminen (1999) Electron microscopic stereological study of collagen fibrils in bovine articular cartilage: Volume and surface densities are best obtained indirectly (from length densities and diameters) using isotropic uniform random sampling. J Anat *195:* 281–293.

Linn, F.C., L. Sokoloff (1965) Movement and composition of interstitial fluid of cartilage. Arthritis Rheum *8:* 481–494.

Maroudas, A. (1976) Transport of solutes through cartilage: Permeability to large molecules. J Anat *122:* 335–347.

Maroudas, A., M. Venn (1977) Chemical composition and swelling of normal and osteoarthrotic femoral head cartilage. II. Swelling. Ann Rheum Dis *36:* 399–406.

McCall, J.G. (1969) Load deformation response of the microstructure of articular cartilage; in Wright, V. (ed): Lubrication and Wear in Joints. London, Sector Publishing, pp 39–56.

Meachim, G., G. Bentley (1978) Horizontal splitting in patellar articular cartilage. Arthritis Rheum *21:* 669–674.

Mow, V.C., M.C. Gibbs, W.M. Lai, W.B. Zhu K.A. Athanasiou (1989) Biphasic indentation of articular cartilage. 2. A numerical algorithm and an experimental study. J Biochem *22:* 853–861.

Mow, V.C., S.C. Kuei, W.M. Lai, C.G. Armstrong (1980) Biphasic creep and stress relaxation of articular cartilage in compression: Theory and experiments. J Biomech Eng *102:* 73–84.
Mow, V.C., W.M. Lai, M.D. Holmes (1982) Advanced theoretical and experimental techniques in cartilage research; in Huiskes, R., D.H. van Campen, J.R. de Wijn (eds): Biomechanics: Principles and Applications. The Hague, Nijhoff, pp 47–74.
Nötzli, H., J. Clark (1997) Deformation of loaded articular cartilage prepared for scanning electron microscopy with rapid freezing and freeze-substitution fixation. J Orthop Res *15:* 76–86.
O'Connor, P., C.R. Orford, D.L. Gardner (1988) Differential response to compressive loads of zones of canine hyaline articular cartilage: Micromechanical, light and electron microscopic studies. Ann Rheum Dis *47:* 414–420.
Oloyede, A., N.D. Broom (1994) Complex nature of stress inside loaded articular-cartilage. Clin Biomech *9:* 149–156.
Orford, C.R., D.L. Gardner (1985) Ultrastructural histochemistry of the surface lamina of normal articular cartilage. Histochem J *17:* 223–233.
Poole, C.A., M.H. Flint, B.W. Beaumont (1984) Morphological and functional interrelationships of articular-cartilage matrices. J Anat *138:* 113–138.
Proctor, C.S., M.B. Schmidt, R.R. Whipple, M.A. Kelly, V.C. Mow (1989) Material properties of the normal medial bovine meniscus. J Orthop Res *7:* 771–782.
Richards, R.G., I. Gwynn (1995) Backscattered electron imaging of the undersurface of resin-embedded cells by field-emission scanning electron microscopy. J Microsc *177:* 43–52.
Richards, R.G., M.J. Kääb (1996) Microwave-enhanced fixation of rabbit articular-cartilage. J Microsc *181:* 269–276.
Romeis, B. (1989) Untersuchung des Binde- und Stützgewebes; in Böck, P. (ed): Romeis Mikroskopische Technik. Munich, Urban & Schwarzenberg, pp 491–566.
Simon, W.H., S. Friedenberg, S. Richardson (1973) Joint congruence. A correlation of joint congruence and thickness of articular cartilage in dogs. J Bone Joint Surg Am *55:* 1614–1620.
Takei, T. (1979) Deformation of the articular cartilage and joint space of the human knee joint under static load. Nippon Seikeigeka Gakkai Zasshi *53:* 577–593.
Takei, T., S. Kobayashi, R. Yagi, N. Mamiya (1986) The structural response of articular-cartilage to compressive load – scanning electron-microscopic study. Scand J Rheumatol *S60:* 29.
Tepic, S., K. Ito (1997) Orientation mechanisms of collagen; in Schneider E. (ed): Biomechanik des menschlichen Bewegungsapparates. Berlin, Springer, pp 204–214.
Weiss, C. (1973) Ultrastructural characteristics of osteoarthritis. Fed Proc *32:* 1459–1466.